J Mater Sci: Mater Electron (2012) 23:425–430
DOI 10.1007/s10854-011-0498-3

Electrical conduction properties of Co-doped ZnO nanocrystalline thin films

A. Yildiz · B. Yurduguzel · B. Kayhan · G. Calin · M. Dobromir · F. Iacomi

Received: 2 June 2011 / Accepted: 11 August 2011 / Published online: 23 August 2011

Abstract The temperature dependent conductivity behavior of 15% Co and 25% Co-doped ZnO nanocrystalline thin films prepared by spin-coating method was examined. It was found that the conductivity shows a change when the Co concentration varies from 15 to 25%. The observed increase of conductivity with increasing Co concentration was interpreted through the grain boundary conduction model. The temperature dependent conductivity of the films was analyzed in term of formulas in consistence with grain boundary conduction model. With rising temperature for 25% Co doped ZnO, a transition from the region in which crystallites are only partially depleted to the region in which the crystallites are entirely depleted was observed around 375 K. Some improtant electrical parameters were determined for the films.

1 Introduction

ZnO with a wide-band-gap (E_g >3 eV) is one of the excellent semiconductors which can be applied to light emitting diodes, solar cells, and gas sensors [1–3]. Among metal oxides, ZnO has been studied intensively due to its rich physical properties. Studies on doping effect on physical properties of ZnO with transitional metals like Co, Ni, and Mn have huge research interests [4]. Efforts are being made to obtain Co doping effect on electrical conductivity of ZnO [4–6]. To date, there have only been a few attempts to explain electrical conduction mechanism in Co-doped ZnO [4–6].

To overcome the lack of studies explaining the electrical conduction in ZnO, it is necessary to correctly determine kinds of electrical conduction mechanism and improve the electrical conductivity to obtain better materials for various applications. In polycrystalline form of ZnO, occurrence of grain boundary (GB) conduction [7–9] due to trapping of the mobile carriers at the grain boundaries (GBs) should be investigated, which may perform polycrystalline materials to be superior candidates over the single crystalline thin film materials. Besides this, various mechanisms working in different temperature regimes need also to be identified to get a clear understanding of electrical conduction in such materials.

In order to investigate all these aspects and study the electrical conductivity behavior on the polycrystalline form of ZnO, we have carried out a comprehensive study of electrical conduction on Co-doped ZnO nanocrystalline thin films. Therefore, thorough investigations of such properties would be rewarding before its utilization in various device applications.

2 Experimental

Co-doped ZnO thin films were deposited by using spin coating method. The zinc acetate and cobalt acetate solutions in N–N-dimethylformamide (2 g metal acetate in 10 ml DMF) were mixed in order to have the Co/(Co + Zn) ratios 0.15 and 0.25. All the used chemicals were of analytical grade. Microscope glass slides were used as substrates for thin film depositions. The deposition process involved depositing a small volume of a certain

A. Yildiz (✉) · B. Yurduguzel · B. Kayhan
Department of Physics, Faculty of Science and Arts, Ahi Evran University, 40040 Kirsehir, Turkey
e-mail: yildizab@gmail.com

G. Calin · M. Dobromir · F. Iacomi
Faculty of Physics, Alexandru Ioan Cuza University, 11 Carol I Blvd., 700506 Iasi, Romania

solution onto the center of a glass substrate and then spinning with a speed of 1,000 rpm during 30 s. After spinning, the thin films were annealed at 373 K for 1 min. The procedure was repeated 10 times. Finally, the as-obtained spin-coated films were annealed at 673 K for 90 min in order to evaporate the residual solvent from the films and to obtain oxide nanocrystalline thin films. Thin film thicknesses were measured by using a DEKTAK profilometer and were found to be around 150 nm.

Structural phase identification of the films was carried out by grazing angle X-ray diffraction technique with CuK_α radiation ($\lambda = 1.5418$ Å, Shimadzu LabX XRD-6000). Compositional analysis of the thin film surface was conducted using X-ray photoelectron spectroscopy (XPS PHI VERSA PROBE 5000, Al K_α source, 1486.6 eV). Charge neutralization was used for all samples. Charge referencing was used for all spectra by applying charge correction to the saturated hydrocarbon C 1s peak at the binding energy of 284.6 eV. Transmittance spectra were registered by mean of a STEAG ETA-OPTIK spectrophotometer in the wavelength range 300–1900 nm.

The tempereature dependence of electrical conductivity was investigated in a temperature range $\triangle T = 300$–425 K by using a two point arrangement and Keithley instruments.

3 Results and discussion

The grazing angle X-ray diffraction (GAXRD, $\alpha = 1°$, scanning rate of 0.04°/s) patterns of undoped and Co-doped ZnO films are shown in Fig. 1. The pattern reveals that the films are polycrystalline in nature. The films exhibit the

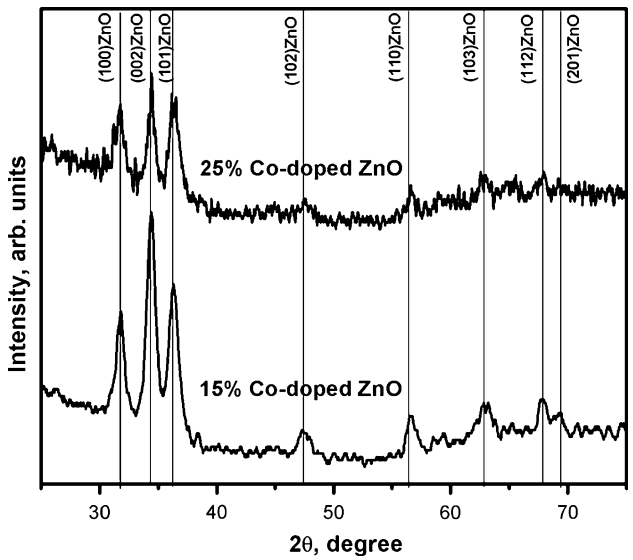

Fig. 1 XRD patterns of Co-doped ZnO thin films

Table 1 Thin film structural characterization

Co content (at %)	a (nm)	c (nm)	I_{100}/I_{002}	I_{101}/I_{002}	L (nm)
15.0	0.3249	0.5204	0.44	0.70	11.44
25.0	0.3245	0.5212	0.92	1.00	14.32

(100), (002) and (101) peaks. The relative intensity of the peaks changes with Co doping concentration. An increase in Co content determines an increase in I_{100}/I_{002} and I_{101}/I_{002} X-ray intensity ratios (Table 1). With the increase of Co concentration, the (002) XRD peak position shifts slightly towards high angles.

Considering the fact that the effective ionic radius (0.058 nm) of Co^{2+} in tetrahedral configuration is close to that of Zn^{2+} (0.060 nm), it is natural that the variation of the position of the (002) diffraction peak with Co concentration is small. Unit cell parameter values as determined by using XLAT-Cell Parameter Refinement software indicate a small diminution in "a" parameter value and a small increase in "c" parameter value confirming that Co ions entered into ZnO lattice merely by substitution (Table 1). This is also an indication that within this composition range, the Co atoms are soluble in ZnO [10, 11].

The grain size (L) of the films was calculated from the full-width at half-maximum (FWHM) of (002) XRD peak using Scherrer formula [12];

$$L = \frac{0.9\lambda}{B\cos\theta} \quad (1)$$

where B is the full-width at half-maximum (FWHM) of (002) diffraction peak, θ is Bragg angle and λ is the X-ray wavelength, respectively. The calculated values of the L are given in Table 1.

The XPS spectra analysis confirmed that the concentration of Co on the surface of the Co-doped ZnO thin films is very close to 15 at % and 25 at %. XPS investigations evidenced that Zn is in 2^+ valence state as the binding energy position of Zn 2p spectra is close to the standard data of zinc oxide (Fig. 2a) [13, 14]. It can be seen that the intensity of the peaks of Zn 2p are decreasing indicating that the Co doping content is increasing, in agreement with Co 2p XPS spectra. Figure 2b shows the Co 2p XPS spectrum of 15% Co-doped ZnO thin film. The difference of binding energies between the $2p_{3/2}$ and $2p_{1/2}$ levels is about 15.5 ± 0.1 eV, which corresponds well with the value for Co^{2+} homogeneously surrounded by oxygen tetrahedra [15, 16].

O1s XPS spectra can be considered as a result of superposition of three XPS peaks (Fig. 2c) having binding energy positions at 528.60, 529.90 and 531.10 eV. The first O1s peak, attributed to O^{2-} ions surrounded by Zn atoms in

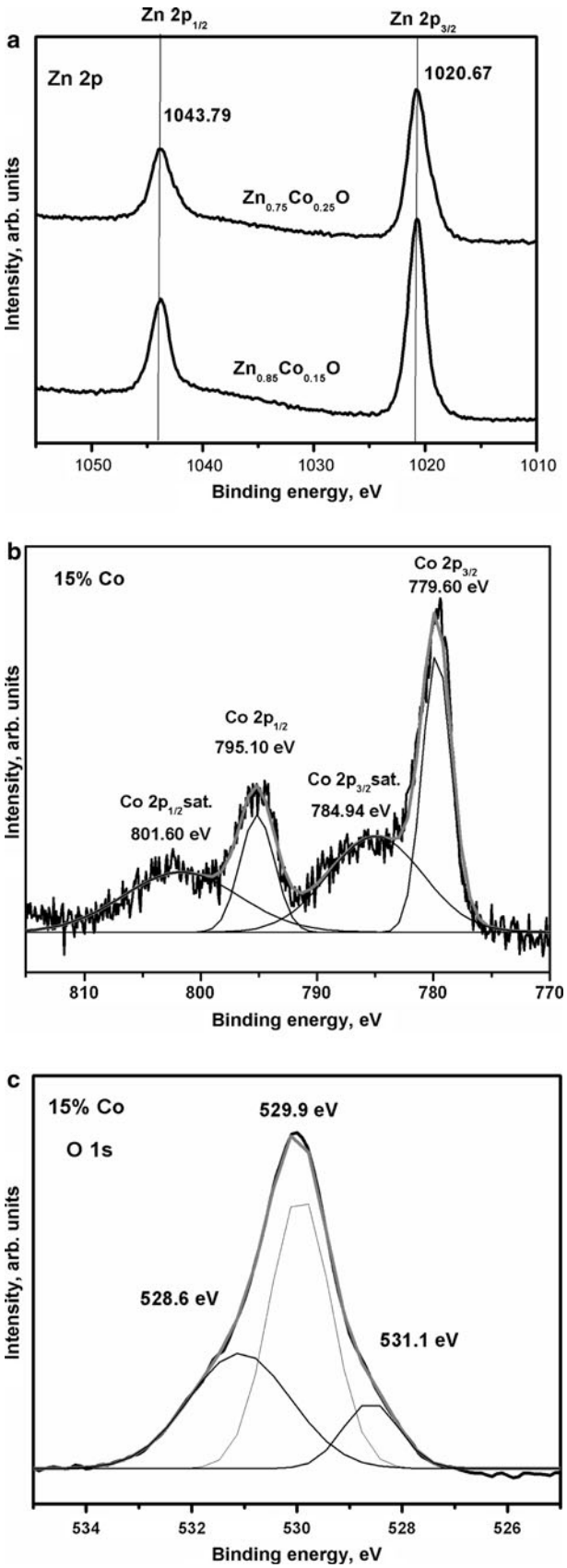

◀ **Fig. 2** XPS spectra: **a** Zn 2p XPS spectra of Co-doped ZnO thin films; **b** Co 2p XPS spectrum of 15% Co-doped ZnO thin film; **c** O1s XPS spectrum of 15% Co-doped ZnO thin film

the wurtzite structure, the second O1s peak, attributed to O^{2-} ions in oxygen deficient regions within the matrix of ZnO, and the third one, attributed to the presence of loosely bound oxygen species or hydroxyl groups on the surface of the films [17, 18].

The optical band gaps of the thin films (E_g) have been determined by evaluating the fundamental absorption coefficient (α) from transmittance spectra, using $\alpha = (\ln T^{-1})/t$, where t is the film thickness and T is the transmittance. In the direct transition semiconductor, the α and the E_g are related by

$$\alpha h\nu = A\left(h\nu - E_g\right)^{1/2} \quad (2)$$

where $h\nu$ is the photon energy, E_g the optical band gap energy and A is a constant. The typical plot of $(\alpha h\nu)^2$ versus $h\nu$ is depicted in Fig. 3. The linear dependence of α^2 versus $h\nu$ indicates that the films are direct transition-type semiconductors. The linear portion is extrapolated to $\alpha = 0$, on energy axis, which gives the E_g of 3.12 and 3.04 eV for 15% Co-doped and 25% Co-doped ZnO films, respectively.

Since the XRD measurements revealed that the films are polycrystalline in nature, we can take into account the applicability of the GB conduction model to our experimental electrical conductivity data. Fig. 4 presents the conductivity–temperature ($\sigma - T$) characteristics of the films, where the plots were carried out by considering the GB conduction model [7–9] in order to compare the σ-T curves of different films in one figure. The conductivity of the 15% Co doped ZnO is $\sim 2.94 \times 10^{-6}\ \Omega^{-1}\ cm^{-1}$ at 325 K, which is much lower than $5.56 \times 10^{-6}\ \Omega^{-1}\ cm^{-1}$ of 25% Co doped ZnO. The films display different $\sigma - T$ properties. The trends in Fig. 4 suggest that there are two types of conduction mechanism contributing to the conductivity in

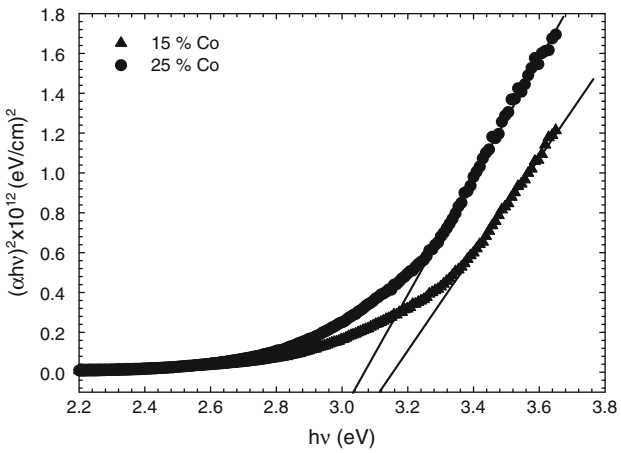

Fig. 3 Plot of $(\alpha h\nu)^2$ versus $h\nu$ for the films

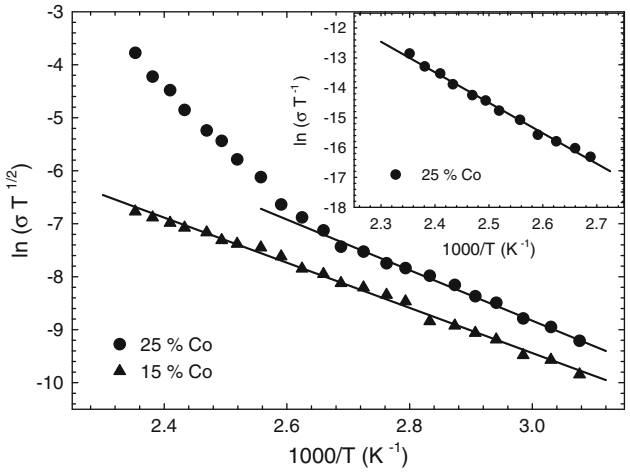

Fig. 4 Temperature dependence of the electrical conductivity plotted as ln ($\sigma T^{1/2}$) versus $10^3/T$ for the films. *Solid lines* are the best-fit *lines* with Eq. 3. The inset of Fig. 4 represents the conductivity of 25% Co-doped ZnO film plotted as ln (σT^{-1}) versus $10^3/T$. *Solid line* is the best-fit *line* with Eq. 5

different temperature ranges for 25% Co doped ZnO. Moreover, a single conduction law can fit the entire curve of the conductivity for 15% Co doped ZnO.

The electrical conduction in the polycrystalline materials is governed by the electron motions between the GBs. According to the GB conduction model, the variation of electrical conductivity with temperature depends on whether the grains are fully depleted or partially depleted of charge carriers. Since the undoped ZnO is a n-type material, we can suppose that donor concentration is N_d. According to GB model [7–9], a critical value of impurity concentration (N_d*) can be defined. In the first case $N_d > N_d$*, the grains are only partially depleted. In this regime, the electrical conductivity can be expressed as [7, 8],

$$\sigma = \left(\frac{Le^2 n v_c}{k_B T}\right) \exp\left(-\frac{E_b}{k_B T}\right), \tag{3}$$

where n is the electron concentration in neutral region of crystallites, e is the electron charge, k_B is the Boltzmann's constant, E_b is the barrier energy at boundary. E_b is described as [7–9],

$$E_b = \frac{L^2 e^2 N_d}{8\varepsilon}, \tag{4}$$

where ε (=8.5) is the low frequency dielectric constant.

For $N_d < N_d$*, the grains are entirely depleted, and Fermi level energy (E_F) becomes aligned with respect to E_F at the interface. In this regime, the conductivity is given as [9],

$$\sigma = \left[\frac{L^2 e^2 N_c N_d v_c}{2k_B T(N_t - LN_d)}\right] \exp\left(-\frac{E_a}{k_B T}\right) \tag{5}$$

and N_t is surface trap density and v_c is the collection velocity:

$$v_c = \left(\frac{k_B T}{2\pi m^*}\right)^{1/2}, \tag{6}$$

where m* (=0.3 m_0) is the effective mass of charge carriers and N_c is the conduction band effective density of states which is described as,

$$N_c = 2\left(\frac{2\pi m * k_B T}{h^2}\right)^{3/2} \tag{7}$$

where h is the Planck's constant.

We will firstly focus on the analysis of the temperature dependence of the conductivity at whole and low temperature (T <375 K) regions of 15% Co-doped and 25% Co-doped ZnO films, respectively. In these temperature regions, Eq. 3 can be applicable to experimental data of the films. According to the GB conduction model [7–9], the carrier concentration increases with decrease of temperature because of decreasing contribution of the crystallites to the conductivity. The temperature dependent conductivity data of 15% Co-doped ZnO do not show any evidence of entirely depleted grains; therefore, this effect can be ruled out for this film. As can be seen in Fig. 4, conductivity of 15% Co-doped ZnO monotonously increases with temperature following a dependence proportional to $\ln(\sigma T^{1/2}) - 1000/T$ in the whole temperature range. This clearly suggests that the electrical conduction is controlled by charge carriers which are trapped by partially depleted states for 15% Co concentration. Also, we suppose that this stiuation is considered at low temperatures for 25% Co concentration.

From the slopes of ln $\sigma = f\,(1000/T)$ curves in Fig. 4, the values of the energy barrier (E_b) have been calculated (at employed temperature regions) for both thin films and their values are given in Table 2. The obtained values of E_b are in agreement with values reported for the polycrystalline materials [7–9]. These activation energies suggest that GB conduction, which takes place in GBs, is the dominant mechanism in the films. After the increase in Co concentration, the trapping of mobile electrons decreases because of the reduced barrier potential energy, E_b, and increased grain size. This phenomenon can be responsable by the variations of the $\sigma - T$ characteristic and the raised values

Table 2 Barrier height (E_b), donor concentration (N_d), Debye screening length (L_D), depletion layer width (l_2), and surface trap density (N_t) for the studied films

Co content (at %)	E_b (eV)	N_d (cm^{-3})	L_D (nm)	l_2 (nm)	N_t (cm^{-2})
15.0	0.368	1.06×10^{19}	1.24	4.04	1.21×10^{13}
25.0	0.319	5.85×10^{18}	1.66	5.06	8.37×10^{12}

of conductivity. Consequently, one can state that, for 15% Co doped ZnO, E_b is always higher in the temperature range considered here. Presumably, the higher E_b of 15% Co doped ZnO, being grown under the same prepared conditions with 25% Co-doped ZnO, is caused by a larger number of trapping centers. Note that the values of the N_d were also estimated by utilizing Eq. 4 for the films (Table 2).

In polycrystalline materials, when the grains are only partially depleted, the depletion layer width (l_2) must be lower than L. l_2 is given as,

$$l_2 = L_D\sqrt{E_b/k_BT} \tag{8}$$

where L_D is Debye screening length which is given as [7],

$$L_D = \left(k_BT\varepsilon/e^2N_d\right)^{1/2}, \tag{9}$$

If $L_D < L/2$, potential barriers exist in the GB region due to interface trap states [7]. The films in this study satisfy the conditions $L_D < L/2$ and $l_2 < L$ (Table 2). Knowing E_b and N_d, we can determine the values of N_t from Eq. 10. When l_2 is lower than L, the N_t is given as [7]

$$N_t = \frac{(8\varepsilon N_dE_b)^{1/2}}{e}. \tag{10}$$

The estimated values of N_t are collected in Table 2.

Secondly, we assume that the entirely depleted model, which is expressed in Eq. 5, is valid for T >375 K in 25% Co-doped ZnO. The electrical conduction in the high temperature region (T >375 K) of the 25% Co doped ZnO is governed by the GB conduction in which the grains are entirely depleted. The values of the E_a and N_t deduced from the straight line of the plot of $\ln(\sigma T^{-1})$ versus $10^3/T$ were calculated as 0.88 eV and 7.57×10^{12} cm^{-2}, respectively. Equation 5 gives a well fit to the conductivity data for the film in the considered temperature range (inset of Fig. 4). We can compare the obtained N_t of 25% Co-doped ZnO thin film with the value constructed according to Eq. 5 (Table 2). The result of such a comparison indicates a well agreement. We have also obtained a well agreement of the obtained here and reported N_t values for various polycrystalline materials, which confirms that the GB conduction is the dominant conduction mechanism [7–9, 19, 20].

Finally, the increase in the conductivity with increasing the Co doping can be understood in the light of the GB model [7–9]. As the Co concentration increases, the grain size increases, and this leads to a reduction in the trapping states at GBs (Table 1). Trapping states are capable of trapping free carriers, and, as a consequence, more free carriers become mobilized as trapping states decreases. Therefore, the conductivity increases with increase in Co concentration in the films.

4 Conclusions

The electrical conductivity behavior of the Co-doped ZnO nanocrystalline thin films prepared by spin-coating method were investigated as a function temperature. XRD and XPS studies evidenced that Co entered into ZnO lattice as Co^{2+}. Cobalt doping determined small increases in "c" unit cell parameter and grain sizes.

Measurements of electrical conductivity of the Co-doped ZnO films, in the temperature range of 325–425 K, lead to the conclusion that the GB conduction mechanism is dominant. The trends in the temperature dependent conductivity data suggest that there are two types of conduction mechanism contributing to the conductivity in two different temperature ranges for 25% Co doped ZnO, while a single conduction law prevails in the entire temperature region for 15% Co doped ZnO. The results of the present work clearly demonstrate that the transport properties of Co-doped ZnO nanocrystalline thin films depend strongly on Co concentration and the grain size of the films. The results of the conductivity data indicate the increase in the trapping of carriers process as the Co doping level decreases imposing a decrease in electrical conductivity.

In order to better understand the effect of the increase in the grain size of the films on electrical properties of ZnO nanocrystalline thin films, Co-doped ZnO nanocrystalline thin films exhibiting a transition depending on Co concentration from the region in which crystallites are only partially depleted to the region in which the crystallites are entirely depleted have been investigated in this work apart from a previous one [18]. It should be noted here that although the experimental technique and theoretical investigations in this work are similar to our previous work on Ni-doped ZnO nanocrystalline thin films [18], the obtained results in this work are new and important for Co-doped ZnO nanocrystalline thin films.

Acknowledgments We are thankful to dr. V. Nica for carrying out XRD measurements. This work was supported by the research projects POSDRU/89/1.5/S/49944 and PN II 12-128/2008 ELOTRANSP.

References

1. S.-H. Nam, M.-H. Kim, D.G. Yoo, S.H. Jeong, D.Y. Kim, N.-E. Lee, J.-H. Boo, Surf. Rev. Lett. **1**, 121 (2010)
2. Y. Hamesa, Z. Alpaslan, A. Kösemen, S.E. San, Y. Yerli, Sol. Energy **84**, 426 (2010)
3. R. Khan, H.-W. Ra, J.T. Kim, W.S. Jang, D. Sharma, Y.H. Im, Sens. Actuators B Chem. **150**, 389 (2010)
4. S. Singh, M.S.R. Rao, Phys. Rev. B **80**, 045210 (2009)
5. R. Kumara, N. Khare, Thin Solid Films **516**, 1302 (2008)
6. K.-C. Kim, E.-K. Kim, Y.-S. Kim, Superlattices Microstruct. **42**, 246 (2007)
7. J.Y.W. Seto, J. Appl. Phys. **46**, 5247 (1975)

8. J.W. Orton, M.J. Powel, Rep. Prog. Phys. **43**, 1263 (1980)
9. G. Baccarani, B. Ricco, G. Spandini, J. Appl. Phys. **49**, 5565 (1978)
10. Y.Z. Yoo, T. Fukumura, Z. Jin, K. Hasegawa, M. Kawasaki, P. Ahmet, T. Chikyow, H. Koinuma, J. Appl. Phys. **90**, 4246 (2001)
11. T.A. Schaedler, A.S. Gandhi, M. Saito, M. Ruhle, R. Gambino, C.G. Levi, J. Mater. Res. **21**, 791 (2006)
12. B.D. Cullity, *Elements of X-Ray Diffraction* (Addison-Wesley, Reading, 1978)
13. B. Pandey, S. Ghosh, P. Srivastava, D. Kabiraj, T. Shripati, N.P. Lalla, Physica. E **41**, 1164 (2009)
14. S. Ghosh, P. Srivastava, P.M. Saurav, P. Bharadwaj, D.K. Avasthi, D. Kabiraj, S.M. Shivaprasad, Appl. Phys. A **90**, 765 (2008)
15. H.J. Lee, S.Y. Jeong, C.R. Cho, C.H. Park, Appl. Phys. Lett. **81**, 4020 (2002)
16. M. Tay, Y.H. Wu, G.C. Han, Y.B. Chen, X.Q. Pan, S.J. Wang, P. Yang, Y.P. Feng, J. Mater. Sci.: Mater. Electron. **20**, 60 (2009)
17. L. Wei, Z. Li, W.F. Zhang, Appl. Surf. Sci. **255**, 4992 (2009)
18. A. Yildiz, B. Kayhan, B. Yurduguzel, A.P. Rambu, F. Iacomi, S. Simon, J. Mater. Sci.: Mater. Electron. **22**, 1473 (2011)
19. A. Oprea, N. Barsan, U. Weimar, J. Phys. D: Appl. Phys. **40**, 7217 (2007)
20. G. Harbeke, *Polycrystalline Semiconductors: Physical Properties and Applications* (Springer, Berlin, 1985)